Robust fault detection based on multiple functional series TAR models for structures with time-dependent dynamics

David Avendano-Valencia, Spilios D. Fassois

7th European Workshop on Structural Health Monitoring
July 8-11, 2014. La Cité, Nantes, France

ROBUST FAULT DETECTION BASED ON MULTIPLE FUNCTIONAL SERIES TAR MODELS FOR STRUCTURES WITH TIME-DEPENDENT DYNAMICS

Luis David Avendaño-Valencia[1], **Spilios D. Fassois**[1]

[1] *Stochastic Mechanical Systems & Automation (SMSA) Laboratory. Department of Mechanical Engineering & Aeronautics. University of Patras, GR 265 04 Patras, Greece.*

ldavendanov@upatras.gr; fassois@mech.upatras.gr

ABSTRACT

Vibration-based *Structural Health Monitoring* of operating wind turbines is challenging, as those structures are characterized by complex non-stationary response and are subject to environmental and operational uncertainties. FS-TARMA parameter based methods are ideal for this problem since they are capable of summarizing the non-stationary dynamics within a small parameter set. In this work, robust FS-TARMA parameter based fault detection methods are pursued by including several FS-TARMA models in the estimation of the statistical model used for posterior decision making. Different combination rules for the different FS-TARMA models are defined, analyzed and compared within the problem of vibration based fault detection on operating wind turbines using simulated data obtained from the FAST aeroelastic simulation code. Results demonstrate the improvement in terms of accuracy and reliability provided by the multiple model approach.

KEYWORDS : *non-stationarity, uncertain operating conditions, functional series TARMA, fault detection.*

INTRODUCTION

Vibration-based *Structural Health Monitoring* (SHM) attempts to implement a *Fault Detection and Identification* (FDI) strategy for engineering structures based on the features of the vibration response signals measured along the structure. The particular case of operating wind turbines is challenging, as those structures are characterized by complex non-stationary response, including cyclic and broad non-stationary effects, derived from the rotating blade system, constantly varying wind speed, direction and turbulence levels, as well as other aeroelastic effects [1, 2]. For this reason, the FDI in structures with non-stationary vibration response, like operating wind turbines, is conventionally performed based on features derived from time-frequency or time-scale representations. The FDI is carried out by monitoring the changes of the patterns of time-frequency or time-scale energy distributions. The current state of the structure is determined either by visual inspection, by image-based pattern recognition techniques or by extraction of time-frequency features [3].

Functional-Series Time-dependent ARMA (FS-TARMA) models are ideal for FDI based on non-stationary vibration response signals, in particular when the non-stationary behavior is produced by deterministic operating patterns [4]. Besides, the parametric FS-TARMA methods provide compact, accurate representations that directly capture the underlying non-stationary dynamics and allow the use of the broad class of parametric diagnosis techniques. Explicit use of TARMA models for the FDI problem were initially reported in [5], where two techniques based on the residual sequences and their corresponding variances are proposed for the on-line fault detection based on non-stationary vibration response. More recently, FDI parameter-based methodologies were proposed, using the property that the *least-squares estimated* projection parameter vector of the FS-TAR models is a Gaussian distributed random vector. Being distributed this way, it is possible to define hypothesis tests for the fault detection and identification problems [6]. For the above described FS-TAR model based methods,

only the information corresponding to a single vibration response signal is used to build the statistical model that is the base for the statistical decision making. As a result, the resulting FDI system is prone to provide wrong diagnostics while facing uncertainties derived from different operational or environmental conditions. The performance and robustness of the FDI methods can be largely improved if information corresponding to different environmental and operational conditions is included to build the statistical model used in the FDI methods.

With that purpose in mind, in this work it is attempted to improve the robustness towards uncertain operating and environmental conditions of the *FS-TARMA parameter-based fault detection methods* by including several vibration response signals within the statistical model used in decision making. In the methodology proposed here, a set of FS-TARMA models derived from different vibration response signals available in the *baseline phase*, are combined to reach a decision during the *inspection phase*. Different combination rules based on simple axioms of probability are explored and compared. The proposed fault detection methods are evaluated in the problem of vibration based FDI on operating wind turbines using simulated vibration responses obtained from the FAST aeroelastic simulation code for uncertain wind speeds and turbulence conditions. Results demonstrate the improvement in terms of accuracy and reliability provided by the multiple model FS-TARMA parameter based FDI methods.

1. FS-TARMA PARAMETER BASED FAULT DETECTION

1.1 Problem definition

Let $\mathfrak{s}_o$ designate the structure of interest at its healthy state, and $y_{o_k}[t]$ a vibration response signal measured from the healthy structure. During the initial *baseline phase* a set of M baseline vibration response signals $Y_o = \{y_{o_k}[t]\}$, with $t = 1,\ldots,N$ and $k = 1,\ldots,M$, are provided. Later, in the *inspection phase*, a new *inspection vibration response signal* $y_u[t]$, acquired from the structure in an unknown state, is provided. Then, a decision about the current structural state must be given by comparing the inspection signal $y_u[t]$ with the available information obtained from the set of signals Y_o.

In order to provide an accurate decision, it is necessary to build a representation for the vibration response $y_u[t]$. In the context of this work, since the structure $\mathfrak{s}_o$ is characterized by non-stationary vibration response, then, the signals are represented by means of functional series TARMA models. Besides, it is desirable that the signal set Y_o covers as much of the environmental and operational variability as possible, and that the acquisition is implemented within a previously specified test maneuver so that the baseline and test signals set are *comparable*.

1.2 FS-TARMA modeling

The vibration response signals are represented by the FS-TARMA$(n_a,n_c)_{[p_a,p_c,p_s]}$ model [4]:

$$y_{o_k}[t] = -\sum_{i=1}^{n_a} a_i^{(k)}[t]\cdot y_{o_k}[t-i] + \sum_{i=1}^{n_c} c_i^{(k)}[t]\cdot w_{o_k}[t-i] + w_{o_k}[t], \quad w_{o_k}[t] \sim \texttt{NID}\left(0,\sigma^2_{w(k)}[t]\right) \tag{1a}$$

$$a_i^{(k)}[t] = \sum_{j=1}^{p_a} a_{i,j}^{(k)}\cdot G_{b_a(j)}[t], \quad c_i^{(k)}[t] = \sum_{j=1}^{p_c} c_{i,j}^{(k)}\cdot G_{b_c(j)}[t], \quad \sigma^2_{w(k)}[t] = \sum_{j=1}^{p_s} s_j^{(k)}\cdot G_{b_s(j)}[t] \tag{1b}$$

where, for the k-th signal,

$a_i^{(k)}[t], c_i^{(k)}[t]$: time-dependent AR and MA parameters

$w_{o_k}[t]$: normally identically distributed (NID) innovations sequence

$\sigma^2_{w(k)}[t]$: time-dependent innovations variance

$a_{i,j}^{(k)}, c_{i,j}^{(k)}, s_j^{(k)}$: projection parameters of the AR, MA and innovations variance

$G_{b_a(j)}[t], G_{b_c(j)}[t], G_{b_s(j)}[t]$: functional basis of the AR, MA and innovations variance

and n_a, n_c are the AR and MA orders, and p_a, p_c and p_s are the dimensionalities of the AR, MA and innovations variance functional basis. Using the FS-TARMA representation, the baseline signal $y_{o_k}[t]$ is replaced by the corresponding FS-TARMA model $\mathfrak{m}_{o_k}$, for all $k = 1,\ldots,M$. In turn, each one of the FS-TARMA models $\mathfrak{m}_{o_k}$ is represented by the projection parameter vector

$$\boldsymbol{\vartheta}_{o_k} = \left[a_{1,1}^{(k)} \quad \cdots \quad a_{n_a,p_a}^{(k)} \;\vdots\; c_{1,1}^{(k)} \quad \cdots \quad c_{n_c,p_c}^{(k)} \;\vdots\; s_1^{(k)} \quad \cdots \quad s_{p_s}^{(k)} \right]^T \tag{2}$$

The problem of estimation of the parameter vector and selection of the structure of FS-TAR and FS-TARMA models is analyzed in detail in a recent review provided in [4].

1.3 Definition of the fault detection problem

Let $\mathfrak{M}$ be the set of all possible FS-TARMA models of the structure of interest, and let $\mathfrak{M}_o \subset \mathfrak{M}$ be the subset of FS-TARMA models corresponding to the healthy state. The *fault detection* problem consists on determining whether the FS-TARMA model $\mathfrak{m}_u$, representing the inspection signal $y_u[t]$, belongs to the subset of FS-TARMA models of the healthy state, $\mathfrak{M}_o$. In this sense, the *fault detection* problem is posed in terms of the following binary hypothesis test,

$$\begin{aligned} H_0: &\quad \mathfrak{m}_u \in \mathfrak{M}_o \quad (\mathfrak{m}_u \text{ belongs to the subset } \mathfrak{M}_o) \\ H_1: &\quad \mathfrak{m}_u \notin \mathfrak{M}_o \quad (\text{otherwise}) \end{aligned}$$

which is carried out by means of the following test:

$$\begin{aligned} p(\mathfrak{M}_o|\hat{\boldsymbol{\vartheta}}_u) \geq p_{lim} \quad &\Rightarrow \quad \text{Accept } H_0 \\ p(\mathfrak{M}_o|\hat{\boldsymbol{\vartheta}}_u) < p_{lim} \quad &\Rightarrow \quad \text{Accept } H_1 \end{aligned} \tag{3}$$

where $p(\mathfrak{M}_o|\hat{\boldsymbol{\vartheta}}_u)$ is the probability that the model subset of the current observation is $\mathfrak{M}_o$, given the estimated parameter vector $\hat{\boldsymbol{\vartheta}}_u$, also known as the *posterior* probability, and p_{lim} is some probability threshold. The test defined in Equation (3) is interpreted as follows: "assign the model of the current vibration signal $\mathfrak{m}_u$ to the subset of models from the healthy state $\mathfrak{M}_o$, if the *posterior* probability $p(\mathfrak{M}_o|\hat{\boldsymbol{\vartheta}}_u)$ is larger than the probability value p_{lim}". As can be inferred, the key quantity in the solution above for the fault detection problem is the *posterior* probability $p(\mathfrak{M}_o|\hat{\boldsymbol{\vartheta}}_u)$. In practice, the posterior probability must be reconstructed from the set models of the baseline vibration response signals $\{\mathfrak{m}_{o_k}\}$. In the sequel, different approaches to obtain robust approximations of $p(\mathfrak{M}_o|\hat{\boldsymbol{\vartheta}}_u)$ based on the set of baseline models $\{\mathfrak{m}_{o_k}\}$ are discussed.

1.4 Estimation of the posterior probability

Sum rule: Provided that the available baseline model set $\{\mathfrak{m}_{o_k}\}$ contains a large enough number of elements embracing most of the possible variability, then $\mathfrak{M}_o \approx \bigcup_{k=1}^{M} \mathfrak{m}_{o_k}$. Then, the posterior probability can be approximated by combining the individual models as follows:

$$p(\mathfrak{M}_o|\hat{\boldsymbol{\vartheta}}_u) \approx p\left(\bigcup_{k=1}^{M} \mathfrak{m}_{o_k} \middle| \hat{\boldsymbol{\vartheta}}_u \right) = \sum_{k=1}^{M} p(\mathfrak{m}_{o_k}|\hat{\boldsymbol{\vartheta}}_u) \tag{4}$$

where $p(\mathfrak{m}_{o_k}|\hat{\boldsymbol{\vartheta}}_u)$ is the probability that the true model is $\mathfrak{m}_{o_k}$ after having observed the (estimated) parameter vector $\hat{\boldsymbol{\vartheta}}_u$ corresponding to the inspection signal. For this rule it is assumed that all the baseline TARMA models $\mathfrak{m}_{o_k}$ are mutually exclusive, namely the true model can correspond **only to one** of the baseline models $\mathfrak{m}_{o_k}$. Then, the joint conditional probability of the model set $\mathfrak{M}_o$ is equal to the sum of all the individual probabilities.

Max rule: A simplified version of the previous rule is obtained when the posterior probability of $\mathfrak{M}_o$ is approximated by the largest posterior probability of $\mathfrak{m}_{o_k}$, namely:

$$p(\mathfrak{M}_o|\hat{\boldsymbol{\vartheta}}_u) \approx \max_k p(\mathfrak{m}_{o_k}|\hat{\boldsymbol{\vartheta}}_u) \tag{5}$$

As in the *sum rule*, it is also assumed that all the TARMA models are mutually exclusive, but in this case, only the model that provides the maximum probability is considered.

Product rule: Let $\hat{\mathfrak{m}}_{o_k}$ a subset of *feasible* models for the signal $y_{o_k}[t]$ obtained after estimation. Thus, for all the baseline signals, a corresponding set of subsets $\{\hat{\mathfrak{m}}_{o_k}\}$ is available. The most reliable models for the vibration response signals of the healthy structure are those contained in the intersection of all the subsets $\hat{\mathfrak{m}}_{o_k}$. Therefore, the posterior probability can be approximated as follows

$$p(\mathfrak{M}_o|\hat{\boldsymbol{\vartheta}}_u) \approx p\left(\bigcap_{k=1}^{M} \hat{\mathfrak{m}}_{o_k} \middle| \hat{\boldsymbol{\vartheta}}_u\right) = \prod_{k=1}^{M} p(\hat{\mathfrak{m}}_{o_k}|\hat{\boldsymbol{\vartheta}}_u) \tag{6}$$

For this rule it is assumed that all the TARMA model subsets $\hat{\mathfrak{m}}_{o_k}$ are independent and thus their joint probability corresponds to the product of the probabilities of the individual subsets.

Now, by using the Bayes rule, the posterior probability $p(\mathfrak{m}_{o_k}|\hat{\boldsymbol{\vartheta}}_u)$ can be written as

$$p(\mathfrak{m}_{o_k}|\hat{\boldsymbol{\vartheta}}_u) \propto p(\hat{\boldsymbol{\vartheta}}_u|\mathfrak{m}_{o_k}) \cdot P(\mathfrak{m}_{o_k}) \tag{7}$$

where, $p(\hat{\boldsymbol{\vartheta}}_u|\mathfrak{m}_{o_k})$ is the probability that estimated parameter vector of the FS-TARMA model of the current observation $\hat{\boldsymbol{\vartheta}}_u$ are the parameters of the the baseline FS-TARMA model $\mathfrak{m}_{o_k}$, and $P(\mathfrak{m}_{o_k})$ represents the prior probability of the individual FS-TARMA model $\mathfrak{m}_{o_k}$, which must satisfy $\sum_{k=1}^{M} P(\mathfrak{m}_{o_k}) = 1$. The prior probabilities indicate which models are more likely to appear, and can be used to adjust a bias towards a model or a certain group of models that are more reliable. If all models are considered to be equally probable, then $P(\mathfrak{m}_{o_k})$ is set to $1/M$.

1.5 Definition of the fault detection methods

To proceed with the fault detection, it is necessary to specify the actual form of the PDF $p(\hat{\boldsymbol{\vartheta}}_u|\mathfrak{m}_{o_k})$ for the sum and max rule, and $p(\hat{\boldsymbol{\vartheta}}_u|\hat{\mathfrak{m}}_{o_k})$ for the product rule. According to [7], the *Weighted Least Squares* (WLS) estimated parameter vector $\hat{\boldsymbol{\vartheta}}_{o_k}$ is Gaussian distributed with mean $\bar{\boldsymbol{\vartheta}}_{o_k}$ (the true parameter vector) and covariance matrix $\boldsymbol{\Sigma}_{\vartheta_{o_k}}$. In this sense, $p(\hat{\boldsymbol{\vartheta}}_u|\mathfrak{m}_{o_k}) = \mathcal{N}(\bar{\boldsymbol{\vartheta}}_{o_k}, \boldsymbol{\Sigma}_{\vartheta_{o_k}})$. However, since the true values of the mean and covariance are unknown, these can be replaced, in the FS-TAR case, by their respective WLS estimates $\hat{\boldsymbol{\vartheta}}_{o_k}$ and

$$\hat{\boldsymbol{\Sigma}}_{\vartheta_{o_k}} = \left(\frac{1}{N}\sum_{t=1}^{N} \frac{\boldsymbol{\phi}_k[t] \cdot \boldsymbol{\phi}_k^T[t]}{\sigma_k^2[t]}\right)^{-1} \cdot \left(\frac{1}{N}\sum_{t=1}^{N} \frac{\hat{\sigma}_{w(o_k)}^2[t] \cdot \boldsymbol{\phi}_k[t] \cdot \boldsymbol{\phi}_k^T[t]}{\sigma_k^4[t]}\right) \cdot \left(\frac{1}{N}\sum_{t=1}^{N} \frac{\boldsymbol{\phi}_k[t] \cdot \boldsymbol{\phi}_k^T[t]}{\sigma_k^2[t]}\right)^{-1} \tag{8}$$

where $\boldsymbol{\phi}_k[t]$ is the regression vector of the k-th model at time t, and $\sigma_k^2[t]$ are the weights used by the WLS estimator for the k-th model ($\sigma_k^2[t] \equiv 1$ in the Ordinary Least Squares case), and $\hat{\sigma}_{w(k)}^2[t]$ is the estimated innovations variance (see details in [6]). Similar expressions can be found for the FS-TARMA case [8]. According to this, the PDF $p(\hat{\boldsymbol{\vartheta}}_u|\mathfrak{m}_{o_k}) \approx p(\hat{\boldsymbol{\vartheta}}_u|\hat{\mathfrak{m}}_{o_k}) = \mathcal{N}(\hat{\boldsymbol{\vartheta}}_{o_k}, \hat{\boldsymbol{\Sigma}}_{\vartheta_{o_k}})$ is replaced on the different combination rules, and after using Equation (3), leads to the fault detection methods summarized in Table 1, for which

$$d_M(\hat{\boldsymbol{\vartheta}}_u, \hat{\boldsymbol{\vartheta}}_{o_k}) = \sqrt{(\hat{\boldsymbol{\vartheta}}_u - \hat{\boldsymbol{\vartheta}}_{o_k})^T \cdot \boldsymbol{\Sigma}_{\vartheta_{o_k}}^{-1} \cdot (\hat{\boldsymbol{\vartheta}}_u - \hat{\boldsymbol{\vartheta}}_{o_k})} \tag{9}$$

is the Mahalanobis distance between the current estimated parameter vector $\hat{\boldsymbol{\vartheta}}_u$ and the estimated parameter vector of the k-th baseline model $\hat{\boldsymbol{\vartheta}}_{o_k}$. Notice that in the product rule and max rule fault detection methods, the negative logarithm has been used and the constant terms have been removed in order to yield simpler expressions.

Table 1 : Tests for fault detection based on multiple FS-TARMA models

Method	Test		
Sum rule fault detection	$\sum_{k=1}^{M} p(\hat{\boldsymbol{\vartheta}}_u \mid \mathfrak{m}_{o_k}) \cdot P(\mathfrak{m}_{o_k}) \geq \alpha$	$\Rightarrow$	accept H_o
	otherwise	$\Rightarrow$	accept H_1
Product rule fault detection	$\sum_{k=1}^{M} d_M^2(\hat{\boldsymbol{\vartheta}}_u, \hat{\boldsymbol{\vartheta}}_{o_k}) \leq \beta$	$\Rightarrow$	accept H_o
	otherwise	$\Rightarrow$	accept H_1
Max rule fault detection	$\min_k \left(\ln \lvert \boldsymbol{\Sigma}_{\vartheta_{o_k}} \rvert + d_M^2(\hat{\boldsymbol{\vartheta}}_u, \hat{\boldsymbol{\vartheta}}_{o_k}) \right) \leq \beta$	$\Rightarrow$	accept H_o
	otherwise	$\Rightarrow$	accept H_1

In summary, the sum rule fault detection method assigns the inspection signal to the healthy state if the (weighted) average probability that its corresponding TARMA parameter vector belongs to one of the models $\mathfrak{m}_{o_k}$ is larger than the fault detection threshold α. The product rule fault detection methods assigns the inspection signal to the healthy state if the average "probabilistic distance" between the corresponding TARMA parameter vector $\boldsymbol{\vartheta}_u$ and $\hat{\boldsymbol{\vartheta}}_{o_k}$ is lower than the fault detection threshold β. In a similar form, the max rule assigns the inspection signal to the healthy state if the minimum "probabilistic distance" is lower than the fault detection threshold β. In all cases, the decision is biased by the prior probabilities $P(\mathfrak{m}_{o_k})$. The simple model case is obtained when only a single model is available, and is equivalent to the method explained previously in [6].

2. EXPERIMENTAL FRAMEWORK

2.1 Data description

The vibration signals are obtained from a finite element model of a "National Renewable Energy Laboratory (NREL) offshore 5-MW baseline wind turbine" simulated by means of the FAST (Fatigue, Aerodynamics, Structures and Turbulence) wind turbine aeroelastic simulator code [9]. Four virtual accelerometers are located at the tower top in the fore-aft and lateral directions, and in the third blade in the edgewise and flapwise directions. The wind turbine response is simulated based on a rated rotation speed of 12.1 rpm, while the input wind excitation is simulated using a Kaimal turbulence model with a power law wind profile type [1]. The average wind speed is 15 m/s with a standard deviation of 2 m/s and expected value of turbulence intensity of 14% at 15 m/s. During the simulation the wind turbine starts at the rated rotation speed with all the control systems on-line. The analysis period is of 800 s with a sampling frequency of 10 Hz, from which the portion from 100 s to 500 s is used for further analysis. Three types of faults with four increasing levels are considered in the experiment:

• **Fault A - Icing on blade 3:** Formation of ice on the last 10% of the length of the third blade. Four fault levels are simulated by increasing 20%, 40%, 60% and 80% of the blade mass density on the last 10% of the length of the third blade. Each fault level is equivalent to an increase of 0.37%, 0.73%, 1.10% and 1.47% of the total mass of the blade.

• **Fault B - Stiffness reduction on blade 3:** Reduction of the overall blade edge stiffness. Four fault levels are simulated by decreasing 5%, 10%, 15% and 20% the blade edge stiffness.

• **Fault C- Stiffness reduction on the tower:** Reduction of the overall stiffness of the tower in the fore-aft and lateral degrees of freedom. Four fault levels are simulated by decreasing 5%, 10%, 15% and 20% the tower stiffness.

For each fault level and for the healthy state, 50 realizations of the wind turbine response are simulated with the FAST code using different seeds for the generation of the turbulence time series. The FS-TAR models of the vibration response signals of the healthy state are identified following the guidelines provided in [2], using a trigonometric functional basis, defined as follows

$$G_{b(1)}[t] = 1, \qquad G_{b(2j)}[t] = \cos[j\omega_o t], \qquad G_{b(2j+1)}[t] = \sin[j\omega_o t], \qquad j = 1,\ldots,(p_a-1)/2$$

where $t = 1,2,\ldots,N$ and $\omega_o = 2\pi f_o/f_s$, with f_o being the rotor angular speed and f_s the sampling frequency, both in Hertz. The obtained FS-TAR model structures are summarized in Table 2.

Table 2 : Identified FS-TAR models of the wind turbine vibration response at different sensor locations.

Sensor	Model structure	RSS/SSS [%]	BIC
Tower top – fore-aft direction	$n_a = 12$, $p_a = p_s = 5$	1.08×10^{-3}	-2.95×10^{4}
Tower top – lateral direction	$n_a = 14$, $p_a = p_s = 5$	1.69×10^{-3}	-3.27×10^{4}
Tip blade 3 – flapwise direction	$n_a = 9$, $p_a = p_s = 5$	5.87×10^{-2}	-1.09×10^{4}
Tip blade 3 – edgewise direction	$n_a = 11$, $p_a = p_s = 5$	2.56×10^{-2}	-1.51×10^{4}

2.2 Results

Fault detection is performed using the different proposed methodologies, namely the multiple model method using the sum rule, the product rule and the max rule, and the single model method, as described in [6]. The fault detection thresholds of each method are optimized by cross-validation, in order to evaluate their performance in the presence of unseen data. Thus, the whole set of vibrations from the healthy structure is randomly split into different non-intersecting subsets. Then a single set is used for evaluation, while the remaining ones are used for training of the methods. The procedure is repeated until all the folds are used for training and testing [10, pp. 483-485]. In the end, the overall performance of the methods corresponds to the average in all the subsets.

In the single model method, since it requires only a single vibration signal, then a single signal from the healthy state is drawn for training, while the remaining 49 records are used for evaluation. In the multiple model methods, the healthy dataset is split into 10 subsets, each one containing 5 vibration response signals. Thus, 45 signals from the healthy state are used for training, while the remaining signals are used for evaluation. Besides, the remaining records corresponding to faulty states are also used for evaluation.

The performance of the methods is measured in terms of ROC curves, which display the False Positive Rate (FPR) vs. True Positive Rate (TPR) of the methods as the fault detection threshold increases from the lowest possible (0) up to the maximum value of the test statistic found in the dataset. Table 3 shows a summary of the overall performance of the fault detection methods using FS-TAR and FS-TARMA models. The performance of the fault detection methods is measured in terms of the *Area Under the ROC Curves* (AUC) and the best true negative rate and true positive rate (TPR) obtained after selecting the optimal threshold with the ROC curves.

The results show that the multiple model fault detection method using the sum rule has the best performance among the tested methods. The performance figures of this method show high mean values but also low dispersion compared with the other methods. The multiple model fault detection method using the product rule also shows good results, comparable with those of its counterpart using the sum rule, but is also capable of boosting the performance in the other sensors as well. On the other hand, the single model fault detection method shows inferior results, as it relies only in the information provided by a single vibration signal. Thus, the average performance is not very good, but also larger

dispersion values are evident. Both the sensors at the tower top in the lateral direction and at the blade 3 in the edgewise direction provide the best results among the parameter based methods. The remaining sensors appear to have lower sensitivity to the simulated faults types.

Table 3 : Summary of the performance of the FS-TAR parameter based fault detection methods after cross-validation in the wind turbine based on vibration response signals.

Fault detection method	Perf.	Tower Top Fore-Aft	Tower Top Lateral	Blade 3 Flapwise	Blade 3 Edgewise
Single model	AUC	0.64 ± 0.03	0.91 ± 0.03	0.55 ± 0.06	0.77 ± 0.08
	TNR	0.61 ± 0.37	0.76 ± 0.33	0.51 ± 0.20	0.65 ± 0.22
	TPR	0.55 ± 0.29	0.75 ± 0.17	0.56 ± 0.18	0.66 ± 0.19
Multiple model - sum rule	AUC	0.68 ± 0.09	0.95 ± 0.03	0.60 ± 0.13	0.85 ± 0.09
	TNR	0.60 ± 0.21	0.98 ± 0.06	0.82 ± 0.11	0.72 ± 0.21
	TPR	0.65 ± 0.03	0.82 ± 0.01	0.31 ± 0.02	0.82 ± 0.01
Multiple model - product rule	AUC	0.66 ± 0.08	0.93 ± 0.03	0.60 ± 0.19	0.86 ± 0.10
	TN	0.56 ± 0.21	0.94 ± 0.10	0.70 ± 0.30	0.68 ± 0.19
	TP	0.67 ± 0.05	0.81 ± 0.02	0.51 ± 0.03	0.90 ± 0.03
Multiple model - max rule	AUC	0.66 ± 0.10	0.93 ± 0.04	0.59 ± 0.13	0.87 ± 0.06
	TNR	0.64 ± 0.31	0.96 ± 0.08	0.90 ± 0.14	0.78 ± 0.15
	TPR	0.61 ± 0.01	0.75 ± 0.04	0.32 ± 0.00	0.85 ± 0.00

Performance figures provided in mean plus/minus standard deviation. AUC : Area Under the ROC Curve, TNR : True Negative Rate, TPR : True Positive Rate.

Figure 1 shows the fault detection statistic of the single model and multiple model (sum rule) fault detection methods obtained for the healthy and faulty records, as well as the optimal fault detection threshold level obtained by cross–validation in the Tower Top - Lateral and Blade 3 - Edgewise sensors. The results demonstrate that, as expected, the distances increase for increasing damage levels. Besides, it is evident that the Tower Top - Lateral sensor is more sensitive to fault types A and C, while Blade 3 - Edgewise sensor is more sensitive to faults B and C. Comparing the resulting fault detection statistic values in Figure 1 of the single model and multiple model (sum rule) fault detection methods it is found that the distance among the healthy and faulty sets appears to be larger in the multiple model method, and the dispersion within each structural state is lower in comparison with the single model counterpart. It is also found that both methods are more sensitive for increasing fault magnitudes. The single model fault detection method is less sensitive for early fault progress but reaches acceptable results for fault levels 3 and 4. The multiple model counterpart is much more sensible, and is capable to yield good results at former stages of the fault and reaches a very high performance for advanced stages.

3. CONCLUSIONS

This work discusses the FS-TARMA parameter based fault detection on structures with non-stationary response and operating in varying operational and environmental conditions. Robustness towards uncertainties is provided by using a set of FS-TARMA models derived from signals acquired under different conditions at the structure. The FS-TARMA models are combined using various combination rules corresponding to simple axioms of probability to improve the statistical model used for detection of faults. Improved accuracy and reliability of the multiple model fault detection methods compared with the conventional one, based on single realizations, demonstrate the virtue of the proposed approach.

ACKNOWLEDGMENTS

The support of this work by the EU FP7 ITN project SYSWIND (Grant 238325) is gratefully acknowledged. In addition, the authors are grateful to the Professor Soren R.K. Nielsen for providing the wind

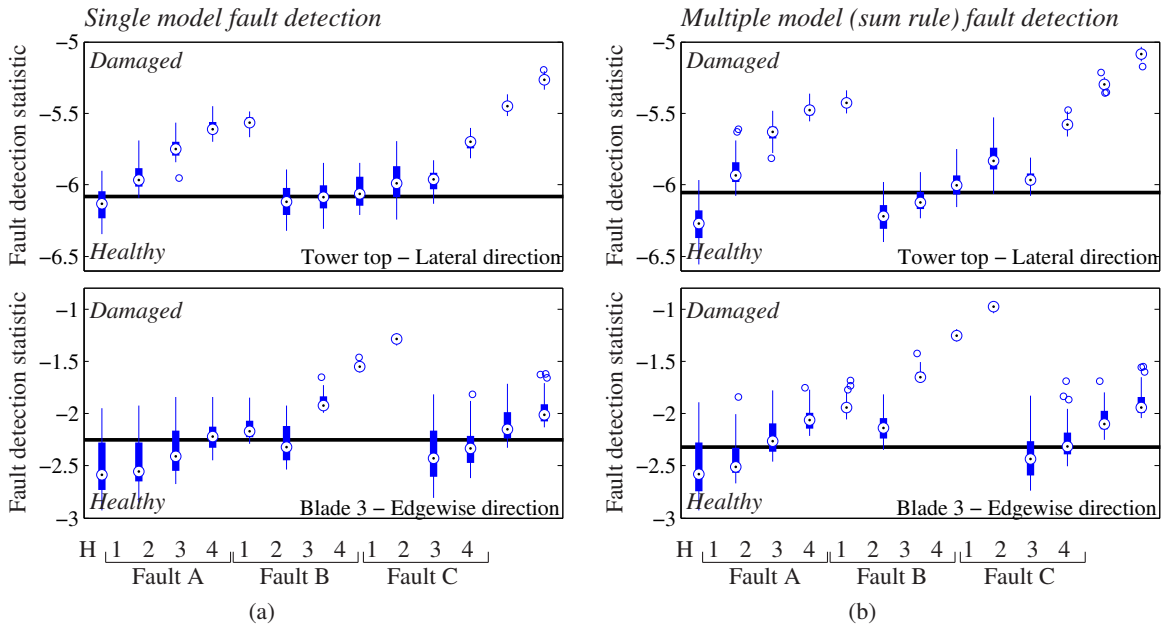

Figure 1 : Boxplots describing the distribution of the fault detection statistic for the (a) single model parameter based method and (b) multiple model (sum rule) parameter based method on the Tower Top - Lateral and Blade 3 - Edgewise sensor locations. The horizontal black line represents the optimal fault detection threshold level obtained after cross–validation.

turbine simulation model and for his useful explanations.

REFERENCES

[1] Morten Hartvig Hansen, J. N. Sorensen, S. Voutsinas, N. Sorensen, and H. Madsen. State of the art in wind turbine aerodynamics and aeroelasticity. *Progress in Aerospace Sciences*, 42:285–330, 2006.

[2] L.D. Avendaño-Valencia and S.D. Fassois. In-operation output-only identification of wind turbine structural dynamics: comparison of stationary and non-stationary approaches. In *Proceedings of the ISMA 2012, Leuven, Belgium*, 2012.

[3] W.J. Staszewski and A.N. Robertson. Time-frequency and time-scale analyses for structural health monitoring. *Phylosophical Transactions of the Royal Society A*, 365:449–477, 2007.

[4] M.D. Spiridonakos and S.D. Fassois. Non-stationary random vibration modelling and analysis via functional series time-dependent ARMA (FS-TARMA) models - a critical survey. *Mechanical Systems and Signal Processing*, 2013.

[5] Aggelos G. Poulimenos and Spilios D. Fassois. Vibration-based on-line fault detection in non-stationary structural systems via statistical model based method. In *Proceedings of the 2nd European Workshop on Structural Health Monitoring*, Munich, Germany, 2004.

[6] M.D. Spiridonakos and S.D. Fassois. An FS-TAR based method for vibration-response-based fault diagnosis in stochastic time-varying structures: experimental application to a pick-and-place mechanism. *Mechanical Systems and Signal Processing*, 38:206–222, 2013.

[7] A.G. Poulimenos and S.D. Fassois. Asymptotic analysis of non-stationary functional series TAR estimators. In *Proceedings of the 15th Mediterranean Conference on Control & Automation*, 2007.

[8] A.G. Poulimenos and S.D. Fassois. Asymptotic analysis of non-stationary functional series TARMA estimators. In *Proceedings of the 15th Symposium on System Identification, SYSID 2009*, 2009.

[9] Jason M. Jonkman and Marshall L. Buhl. FAST user's guide. Technical report, National Renewable Energy Laboratory NREL, 2005.

[10] Richard O. Duda, Peter E. Hart, and David G. Stork. *Pattern Classification*. Wiley, 2nd edition, 2000.